Published in final edited form as:
Glia. 2012 May ; 60(6): 908–918. doi:10.1002/glia.22323.

The CCL2-CCR2 system affects the progression and clearance of intracerebral hemorrhage

Yao Yao and **Stella E. Tsirka**
Program in Molecular and Cellular Pharmacology, Dept of Pharmacological Sciences, Stony Brook University, Stony Brook, NY 11794-8651

Abstract

Intracerebral hemorrhage (ICH) has been associated with inflammation and apoptosis. The CCL2-CCR2 chemotactic system is one of the major signaling pathways that induce inflammation and apoptosis. However, its role on ICH has not been investigated. We subjected wild-type, $CCL2^{-/-}$ and $CCR2^{-/-}$ mice to collagenase-induced ICH, and assessed histological and behavioral outcomes. Lack of CCL2 or CCR2 decreased the hematoma volume early after collagenase-induced ICH, but delayed its recovery. The hematoma size was accompanied by brain edema, neuronal death, and neurological scores. Although microglia activation/migration was attenuated in $CCL2^{-/-}$ or $CCR2^{-/-}$ mice 1 day after injury, more microglia were present at later time points, suggesting that alternative signaling pathways had been activated to recruit them. On the contrary, leukocyte and neutrophil infiltration was decreased in these mice, suggesting a tighter/recovered blood-brain barrier. In addition, we also found that FL- and K104Stop-CCL2 were able to restore the changes found in $CCL2^{-/-}$ mice, but K104A-CCL2 failed to do so. These results suggest that plasmin-mediated truncation of CCL2 may be an indispensable step to fully activate the chemokine *in vivo*. The data also indicate that CCL2-CCR2 signaling pathway may be a molecular target for the treatment of ICH.

Keywords

CCL2; CCR2; Intracerebral Hemorrhage

Introduction

Intracerebral hemorrhage (ICH) constitutes 10–13% of strokes and is usually accompanied with poor prognosis (Ribo and Grotta, 2006, Donnan et al., 2010). Although the ICH pathogenic events are elusive, apoptosis (Matsushita et al., 2000) and inflammation (Castillo et al., 2002) play important roles. When ICH occurs, microglia become activated and secrete inflammatory cytokines and chemokines. The blood-brain barrier (BBB) is disrupted and peripheral leukocytes infiltrate into the brain possibly via chemokine gradients (Lortat-Jacob et al., 2002, Cavcic et al., 2011). The activated microglia and infiltrated leukocytes can modulate ICH progression (Wang et al., 2003, Wang and Tsirka, 2005b, Moxon-Emre and Schlichter, 2011, Provencio et al., 2011).

Monocyte chemoattractant protein-1 (CCL2), a potent chemokine for microglia and monocytes (Yao and Tsirka, 2010, 2011b), is expressed under physiological conditions at low levels in the brain (Sheehan et al., 2007, Ma et al., 2011). Its expression is dramatically

Address correspondence to: Stella Tsirka, Tel: 631-4443859, Fax: 631-4443218, stella@pharm.stonybrook.edu.
The authors declare no conflicts of interest.

increased during excitotoxicity and stroke (Sheehan et al., 2007, Ma et al., 2011). In collagenase-induced ICH, CCL2 expression is elevated in the ipsilateral hemisphere, where it becomes proteolytically processed. Although the source of CCL2 during ICH has not yet been reported, astrocytes may be a major source based on studies on other models (Thompson and Van Eldik, 2009, Semple et al., 2010, Kooij et al., 2011, Nelson et al., 2011). By binding to its receptor CCR2, CCL2 induces the migration and accumulation of monocytes/microglia around lesion sites in brain injuries and excitotoxic lesions (Dimitrijevic et al., 2006). Previous studies in our lab showed that neuronal death and microglial accumulation were attenuated in mice lacking CCL2 or mice injected with CCL2 blocking antibody, suggesting that CCL2 contributes to death via microglial recruitment. In addition, CCL2 promotes BBB compromise (Stamatovic et al., 2003, Stamatovic et al., 2005, Dimitrijevic et al., 2006, Stamatovic et al., 2006), which may enhance leukocyte infiltration into the brain. Plasmin activity is indispensable for CCL2-induced chemotaxis and BBB compromise: (1) plasmin cleaves CCL2 at lysine (K)-104 (Sheehan et al., 2007), (2) the truncated CCL2 has a much higher chemotactic potency than the full length CCL2 (Sheehan et al., 2007, Yao and Tsirka, 2010, 2011b), and (3) the truncated CCL2, not the intact CCL2, induces BBB disruption (Yao and Tsirka, 2011b).

As CCL2 is an important inflammatory mediator and inflammation plays an important role in ICH, we asked if the CCL2/CCR2 system is critical in the ICH events. We compared the ICH outcome in wild-type (wt) mice and mice deficient for CCL2 or CCR2, or delivered back to the deficient mice the missing chemokine and evaluated ICH progression.

Materials and Methods

Animals and cultures

C57BL/6 (wild-type), $CCL2^{-/-}$ and $CCR2^{-/-}$ mice were purchased from Jackson Laboratories and maintained in the Department of Laboratory Animal Research at Stony Brook University (SBU) with free access to water and food. $CCL2^{-/-}$ and $CCR2^{-/-}$ mice have been backcrossed for 12 generations to C57BL/6. Experimental procedures were in accordance to the NIH guide for care and use of animals and the Institutional Animal Care and Use Committee at SBU.

ICH Model

Mice weighting 25–35g were injected with atropine (0.6μg/g of body weight) and avertin (0.02ml/g of body weight) intraperitoneally. A burr hole was drilled (−1 mm posterior to bregma, 3 mm lateral from midline and 4 mm in depth). Collagenase (0.18U in 500nl saline) (Wang et al., 2003, Wang and Tsirka, 2005b) with or without recombinant CCL2 proteins (150ng) was injected into the brain over 5 minutes. The needle remained in place for 2min to prevent reflux. On 1, 3, 7, and 14 days post injury (dpi) mice were transcardially perfused, the brains removed, fixed, dehydrated and sectioned.

Histology

Hematoxylin/eosin (H&E) and luxol fast blue/cresyl violet staining were performed to visualize the hematoma. Briefly, for H&E sections were washed twice in PBS and kept in hematoxylin for 15min at room temperature. They were washed in tap water twice, 70% ethanol with 1% hydrochloride acid for 3 sec, followed by 3 washes in tap water and placed in eosin for 5 sec, washed in PBS, dehydrated in gradient ethanol and mounted. Luxol fast blue/Cresyl violet was also used to visualize the hematoma as described previously (Clark et al., 1998, Wang et al., 2003, Thiex et al., 2004, Wang and Tsirka, 2005b).

For Fluoro-Jade C (FJC) staining (Schmued and Hopkins, 2000) slides were incubated in 1% NaOH in 80% ethanol for 5min, washed in 70% ethanol and distilled water, and incubated in 0.06% $KMnO_4$ for 10min. They were washed in water and transferred to 0.0001% FJC (in 0.1% acetic acid) for 10min. The slides were rinsed in water, dried at 56° *C* for 5min, cleared in xylene for 2min and mounted with DPX. FJC^+ cells were counted in 3 sections/mouse, using 3 fields immediately adjacent to the hematoma at 400X magnification over a microscopic field of $0.01mm^2$. Large blood vessels were avoided. The numbers of degenerating cells were expressed as cells/mm^2 (Wang et al., 2003, Wang and Tsirka, 2005b).

Hemorrhagic Injury Analysis

The injury volumes (Clark et al., 1998, Wang et al., 2003, Thiex et al., 2004, Wang and Tsirka, 2005b) in H&E-stained slides from wt, $CCL2^{-/-}$ and $CCR2^{-/-}$ mice were quantified on 30μm coronal sections using NIS-Elements D3.0. The hemorrhage areas from serial coronal slices were added and the injury volume (mm^3) was calculated: Injury Volume=measured area X slice thickness (30μm).

Immunohistochemistry/immunofluorescence

Microglia/macrophages were visualized using Iba-1 antibody (1:500; Wako Inc) followed by 1:200 biotinylated anti-Rabbit or Alexa-555 anti-Rabbit antibodies for 1-hour at room temperature. The slides were stained with the ABC kit (Vector Labs) and Diaminobenzidine solution. Iba-1^+ cells were counted in 5 slides using 5 random fields immediately adjacent to the hematoma at 400X magnification. Four animals/group/time point were used for quantification. Leukocytes and neutrophils were visualized by anti-CD45 (BD PharMingen) and Ly6G (R&D), respectively, both at 1:500 dilution, followed by Alexa 488-anti-rat antibody (Invitrogen).

Brain Edema Measurement

At days 1 and 7 post collagenase injection, the mice were euthanized, the brains collected and cut into two hemispheres. Cerebellum was used as internal control. The wet weights of the two hemispheres and cerebellum were obtained. The samples were dried for 24-hours and weighted (dry weight). Brain edema was calculated as: Brain Edema=(Wet Weight-Dry Weight)/Wet Weight X100. At this point we can't differentiate between bleeding-induced water increase and secondary edema, as we measure the total water content of the tissue(Wang et al., 2003, Wang and Tsirka, 2005b).

Neurological Deficit

All mice were scored for neurological deficits 1, 3, 7, and 14 dpi using a modified 28-point scoring system (Clark et al., 1998, Wang et al., 2003, Thiex et al., 2004, Wang and Tsirka, 2005b), that includes 6 properties (body symmetry, gait, climbing, circling behavior, front limb symmetry, and compulsory circling), each graded from 0 to 4, establishing a maximum score of 24. The higher the score, the higher the neurological deficit. The person who scored the deficit was blinded to the genotypes/treatments. The individual scores of the mice tested are provided in Supplemental Figure 4.

Statistics

Results are shown as mean±SD. Student's t-test was used to analyze differences between two groups. ANOVA was used when bigger groups were compared. Comparison with day 1 within the same genotype, *$p<0.05$; comparison with wild-type (for Figs. 1–3 and Table A) or $CCL2^{-/-}$ mice injected with FL-CCL2 (for Figs. 4–6 and Table B) at the same time points, #$p<0.05$.

Results

CCL2 or CCR2 deficiency and hematoma volume

Because the CCL2-CCR2 chemokine system is critical for microglial recruitment (Yao and Tsirka, 2010), which play both detrimental and beneficial roles during ICH (Wang et al., 2003, Wang and Tsirka, 2005b, Wang and Dore, 2007), we examined whether lack of CCL2 or CCR2 can affect the hematoma size. We induced hemorrhage in wt mice and $CCL2^{-/-}$ or $CCR2^{-/-}$ mice and examined the outcome at 1, 3, 7, and 14 dpi. The hematoma was visualized by H&E (Figure 1) and luxol fast blue/cresyl violet staining (Supplement Figure 1). In wt mice the hematoma was very large (28.42mm^3) at 1 dpi, and decreased over time (22.2 mm^3 at 3 dpi and 4.26 mm^3 at 7 dpi, and 0.61 mm^3 at 14 dpi). In $CCL2^{-/-}$ and $CCR2^{-/-}$ mice the hematoma size followed a different timecourse. It was smaller at 1dpi (5.01 and 7.27 mm^3, respectively), peaked at 3dpi (12.48 and 20.2 mm^3) and decreased slowly (11.68 and 19.17 mm^3 at 7 dpi and 4.25 and 4.72 at 14 dpi, respectively). These data suggest that CCL2-CCR2 signaling may affect the progression and resolution of the hematoma.

Microglia/Macrophage recruitment and leukocyte infiltration during ICH in CCL2−/− or CCR2−/− mice

We visualized microglia/macrophages recruited to the ICH using Iba-1, a microglia/macrophage marker. There was no difference in baseline microglia numbers among the genotypes (Figure 2). As reported (Wang et al., 2003, Wang and Tsirka, 2005b, Wang and Dore, 2007), Iba-1^+ cells showed large cell bodies and short processes in wt mice at 1dpi and their numbers increased slightly (Figure 2), indicating the transformation towards an activated state. In $CCL2^{-/-}$ and $CCR2^{-/-}$ mice, neither the numbers nor the morphology of Iba-1^+ cells changed. The Iba-1^+ cell density increased at 3dpi in wt mice and $CCL2^{-/-}$ or $CCR2^{-/-}$ mice (Figure 2), suggesting that alternative (CCL2- and CCR2-independent) signaling events may be activated. Although more microglia/macrophages were observed in the penumbra by 7dpi, the intensity of the Iba-1 signal decreased, suggesting potentially that the microglia had started reverting to a resting state. $CCL2^{-/-}$ and $CCR2^{-/-}$ mice by 7dpi, however, showed high density and strong staining of microglia/macrophages, suggesting that the signaling pathway(s) that had been activated in 3dpi was still functional at 7dpi.

Microglial activation was also evaluated using inducible nitric oxide synthase (iNOS) as a marker: iNOS expression was observed at 1dpi, peaked at 3dpi and decreased by 7dpi in wt mice (Figures 3A and B). The expression of iNOS at 1 and 3dpi in CCL2−/− or CCR2−/− mice was similar to wt mice, but by 7dpi the mice still displayed high level of iNOS, which co-localized with Iba-1 at the border of hematoma (Figure 3A).

CCL2 can compromise BBB integrity (Stamatovic et al., 2003; 2005; 2006; Dimitrijevic et al., 2006; Yao and Tsirka, 2011a, b) thus allowing the infiltration of peripheral leukocytes into the brain. We assessed inflammatory cells infiltration using CD45, a pan-leukocyte marker, and Ly6G, a neutrophil marker. Infiltrated $CD45^+$ cells were observed around the hematoma early after ICH (1 and 3dpi, Figure 3C), probably due to collagenase-induced disruption of blood vessels. By 7dpi, the $CD45^+$ signal increased in wt mice, although the hematoma size was smaller, suggesting infiltration of peripheral blood cells at this time point. In $CCL2^{-/-}$ and $CCR2^{-/-}$ mice the $CD45^+$ signal was still low by 7dpi (Figure 3C), suggesting little-to-no infiltration of leukocytes. Neutrophils showed accumulation in wt brains early after injury (1 and 3dpi) and the number decreased significantly by 7dpi (Figure 3D). This neutrophil infiltration time-course was consistent with previous reports (Gong et al., 2000, Xue and Del Bigio, 2000a, b, Peeling et al., 2001, Wang and Tsirka, 2005a). CCL2 and CCR2 deficient mice showed only low neutrophil cell infiltration in the brain,

which did not increase drastically during the ICH time course (Figure 3D). Previously we have shown that CCL2 compromises BBB integrity in a CCR2-dependent manner and there is no difference in baseline BBB leakage among wt, $CCL2^{-/-}$ and $CCR2^{-/-}$ mice under physiological conditions (Yao and Tsirka, 2011b). Together our data suggest that in the absence of CCL2 and/or CCR2 the compromise of BBB may be delayed in collagenase-induced ICH.

Effects of CCL2-CCR2 deficiency on edema, neuronal death, and neurological behavior

Brain edema is an important clinical complication of ICH. We measured the water content in the animals after ICH. Significant increase of brain water was found in the ipsilateral hemisphere in wt mice 1dpi (Table 1A). Mirrored by the hematoma volume, the water content in the ipsilateral side decreased at later time points (3 and 7dpi), suggesting a recovery from ICH. $CCL2^{-/-}$ and $CCR2^{-/-}$ mice showed a trend that followed the progress of ICH. The water contents in the contralateral hemisphere and the cerebellum (the internal control), however, were not affected by the ICH.

ICH-induced neuronal death was visualized using FJC, a dye that specifically labels degenerating neurons (Schmued et al., 1997, Wang and Tsirka, 2005a, b, Bian et al., 2007). Wt mice showed many FJC^+ cells ($387/mm^2$) at 1dpi and the number decreased at 7dpi ($142/mm^2$, Figures 3E and F), as the animals were recovering. $CCL2^{-/-}$ mice showed a lower number ($229/mm^2$) of degenerating neurons at 1dpi, but the numbers increased at 7dpi ($295/mm^2$). $CCR2^{-/-}$ mice followed a similar trend as $CCL2^{-/-}$ mice (200 and 303 FJC^+ cells/mm^2 at 1 and 7dpi, respectively), suggesting that the number of degenerating neurons correlated with hematoma size.

Furthermore, we assessed neurobehavioral changes after ICH. For wt mice the neuronal deficit score was high early after injury but decreased at 7dpi (from 10.9 and 10.1 at 1 and 3dpi, respectively, representing the severity of the injury to 4.7 at 7dpi). $CCL2^{-/-}$ mice showed low neuronal deficit score at 1dpi (7.3) and higher scores at 3 (9) and 7dpi (10.2) (Figure 3G). $CCR2^{-/-}$ mice followed the same trend as $CCL2^{-/-}$ (Figure 3G). The neurological scores decreased for all animals at 14dpi (albeit remaining still higher in $CCL2^{-/-}$ and $CCR2^{-/-}$ mice) indicative of an active recovery process.

Infusion of FL- and plasmin-truncated CCL2 restores wt-phenotype in $CCL2^{-/-}$ mice

Plasmin cleaves CCL2 at K104 enhancing *in vitro* its chemotactic potency and BBB-compromising activity (Sheehan et al., 2007, Yao and Tsirka, 2010, 2011b). To investigate whether CCL2 activation is involved in ICH, we examined whether CCL2 becomes truncated during ICH. Two bands corresponding to full-length (FL) and truncated (Cleaved) CCL2 were detected 6 hours after ICH in the ipsilateral, but not the contralateral, hemisphere, suggesting CCL2 activation after ICH (Supplemental Figure 2). We then infused different recombinant, previously characterized CCL2 proteins (Yao and Tsirka, 2010, 2011a, b) into the brains of $CCL2^{-/-}$ mice and examined the outcome. Since collagenase does not cleave CCL2 (Supplemental Figure 3), we injected CCL2 together with collagenase on day 0 and assessed the pathological changes at 1, 3, and 7dpi. In $CCL2^{-/-}$ mice infused with cleaved K104Stop-CCL2 (constitutively active CCL2), we observed a larger hematoma at 1dpi ($34.35mm^3$) that decreased at 3 and 7dpi (6.08 and $3.21mm^3$, respectively) (Figure 4). Infusion of K104A-CCL2 (plasmin uncleavable CCL2) (Yao and Tsirka, 2010) did not affect the $CCL2^{-/-}$ hematoma characteristics. Like K104Stop-CCL2, FL-CCL2 infusion induced a large hematoma ($12.92mm^3$) at 1dpi and the volume decreased to $1.01mm^3$ at 7dpi (Figure 4). FL-CCL2-infused mice had a smaller hematoma at 1dpi, compared to K104Stop-CCL2-injected mice, suggesting that K104Stop-CCL2 is more potent than FL-CCL2.

Infusion of FL- or K104Stop-CCL2 to CCL2$^{-/-}$ mice restores wt ICH characteristics

Infusion of K104Stop-CCL2 significantly increased microglia/macrophage density in the peri-injury site at 1dpi (Figure 5). Infusion of FL- and K104A-CCL2 did not enhance the density of microglia/macrophages adjacent to the hematoma at 1dpi and the cells showed long processes and lightly-stained cell body, indicating a resting state. By 3dpi, microglia/macrophages exhibited a fully activated morphology (were amoeboid with short processes and intensely-stained cell body) and the numbers of microglia/macrophages increased significantly in all groups (Figure 5). This is consistent with the observation that microglia/macrophages were fully activated in CCL2$^{-/-}$ at 3dpi (Figure 2). By 7dpi in mice injected with FL- and K104Stop-CCL2 a dramatic decrease of Iba-1^{+} numbers was evident, and the cells returned to the resting or semi-activated state (Figure 5). Mice infused with K104A-CCL2 showed consistent activation and high density of microglia/macrophages around the injury site.

The levels of iNOS were similar between wt and CCL2$^{-/-}$ mice (Figure 3). When the recombinant CCL2 proteins were infused, iNOS levels changed: uncleavable K104A-CCL2 infusion induced an increase of iNOS expression over time (Figure 6A, B), whereas infusion of K104Stop-CCL2 resulted in iNOS decrease over time. Similar to K104Stop-CCL2, FL-CCL2 decreased iNOS expression at 7dpi (Figure 6A, B). Together, our data suggest that FL- or K104Stop-CCL2 infusion can revert the microglial activation state observed in CCL2$^{-/-}$ mice.

We examined the CCL2 protein infusion effect into CCL2$^{-/-}$ mice on leukocyte and neutrophil infiltration after ICH. As shown in Figure 6C, infusion of FL-CCL2 or K104Stop-CCL2 yielded a slow increase in CD45^{+} cell infiltration at later time points in the brain parenchyma. The infusion of K104A-CCL2 did not affect the CD45^{+} cell infiltration at any time point examined. Similarly, infusion of FL- and K104Stop-CCL2 significantly enhanced neutrophil infiltration at early time points after ICH and decreased by 7dpi (Figure 6D). K104A-CCL2 infusion did not yield dramatic changes in Ly6G levels (Figure 6D), again suggesting that K104A-CCL2 was not functional active.

We also quantified the effects of these recombinant proteins on edema, neuronal death and behavior of the CCL2$^{-/-}$ mice. Infusion of FL- or K104Stop-CCL2 into the animals resulted in increase of the water content measurements in the ipsilateral hemisphere at the early timepoints after ICH, but was decreased at 7dpi, whereas the infusion of K104A-CCL2 led to increase of water content and accompanying edema over time (Table 1B).

Similarly, the numbers of degenerating neurons were high early after the infusion of FL- or K104Stop-CCL2, but decreased significantly at 7dpi (Figure 6E). These data suggest that it is the truncated fully active CCL2 (K104Stop-CCL2) that more efficiently reverted the phenotype of CCL2$^{-/-}$ mice.

Furthermore, the infusion of FL-CCL2 or K104Stop-CCL2 resulted in a better behavioral over time (10.25 at 1dpi, 8.25 at 3dpi and 5.75 at 7dpi for FL-CCL2, and 11.73 at 1dpi, 8.67 at 3dpi, and 4.25 at 7dpi for K014Stop-CCL2). K104A-CCL2 infusion yielded a low score at 1dpi (5.78) and it increased to 7.67 and 9.75 at 3 and 7dpi, respectively (Figure 6F). Collectively, our data showed that infusion of FL- or K104Stop-CCL2 changed the ICH outcome in CCL2$^{-/-}$ mice and made it comparable to that of wt mice after ICH, underscoring the crucial role of plasmin-mediated truncation of CCL2 on its biological activities *in vivo*.

Discussion

Hemorrhagic stroke, which represents a small percentage of stroke incidents (Qureshi et al., 1997), is an acute and devastating clinical event. Inflammation plays an important role in ICH pathophysiology (Gong et al., 2001, Wang et al., 2003, Wang and Tsirka, 2005b, Xi et al., 2006, Wang, 2010). Activated microglia and infiltrated macrophages accumulate in the peri-hematoma region (Wang et al., 2003, Wang and Tsirka, 2005b, Wang and Dore, 2007). Here we report that CCL2 and CCR2 affect the progression of ICH, as deficiency in the chemokine and chemokine receptor significantly decreased hematoma size at early time points but delayed the recovery. The size of hematoma was paralleled by the water content in the ipsilateral hemisphere and neuronal death at the peri-hematoma region. Consistently, neurobehavioral deficit scores were also mirrored by hematoma size. These data suggest that mice deficient for CCL2 or CCR2 have an initially milder but longer-lasting injury after ICH.

Microglia, as the brain resident immune cells, play a dual role during brain injury: they promote neuronal death by secreting a variety of cytotoxic factors, such as TNF-α and IL-1β (Kim and de Vellis, 2005), and they phagocytose cell debris and injured neurons to enhance recovery (Elkabes et al., 1996). Which role they undertake after ICH is dependent on the time after injury and their local environment. Our data suggest that Iba-1^+ cells may play a detrimental role at early time points (1dpi) in the collagenase-induced ICH model, although their role later is unclear due to the activation of alternative signaling cascades. It should be noted that Iba-1 staining identifies both brain-resident microglia and infiltrating macrophages. We do make the assumption that since collagenase acts locally, the infiltration of macrophages will most likely take place around the site of collagenase injection. Presence of activated Iba1+ cells further away from the lesion area may signify the activation and recruitment of microglia. Immunohistochemistry for iNOS, a functional marker of proinflammatory microglia/macrophages, reveals that the activation of microglia may be directly related to the tissue damage.

Unexpectedly, at later time points after ICH the knockout mice showed higher density of Iba-1^+ cells in the peri-hematoma region, suggesting that signaling pathways distinct from the CCL2-CCR2 system may function to attract microglia/macrophages. We are currently studying the mechanisms underlying such alternative signaling pathways in the chemokine/chemokine receptor KO mice after ICH.

It has been shown that leukocyte infiltration correlates with disruption of BBB (Gurney et al., 2006, Candelario-Jalil et al., 2007, Reijerkerk et al., 2008, Kuang et al., 2009). Consistent with our previous report that CCL2−/− or CCR2−/− mice have a ‘tighter’ BBB, infiltration of peripheral cells was low in these mice at all the time points examined. Since CD45 is also expressed by brain resident microglia, although at low levels, resident microglia may contribute to the $CD45^+$ signal we detected. The number of neutrophils, however, was decreased in both knockout mice early after ICH, suggesting that CCL2-CCR2 may regulate neutrophil infiltration directly or indirectly. Consistent with previous reports that neutrophils are fast-responding cells (Gong et al., 2000, Xue and Del Bigio, 2000a, b), longer (7dpi) timepoints revealed no differences among the three genotypes.

The infusion of CCL2 proteins showed that FL- and K104Stop-CCL2 restored wt phenotype in $CCL2^{-/-}$ mice, whereas plasmin-resistant K104A-CCL2 failed, suggesting that plasmin-mediated truncation is an indispensable step to fully activate CCL2 in vivo. This is consistent with our in vitro data that plasmin-truncated CCL2 has higher biological activities (Yao and Tsirka, 2010, 2011b). Although here we did not infuse recombinant CCL2 proteins in wt mice, we have previously shown (Yao and Tsirka, 2011b) that when we infuse FL- or

active CCL2 (K104Stop-CCL2) in wt animals the integrity of BBB is more readily disrupted. Therefore we would expect that upon overexpression/administration of CCL2 active recombinant proteins into wt mice we would observe a bigger hematoma early after ICH and a delayed recovery.

Due to its early identification and high potency for chemoattraction of mononuclear cells, the CCL2-CCR2 axis has been extensively studied. Some reports suggest that in ischemic stroke, inhibition of the CCL2-CCR2 system ameliorates injury by reducing brain edema, leukocyte infiltration and expression of inflammatory mediators (Dimitrijevic et al., 2007, Tsukuda et al., 2011), indicating a detrimental role of CCL2-CCR2 axis. It should be noted that inflammation can be both detrimental and beneficial, depending on the timing and environment. Other reports showed that the CCL2-CCR2 interaction is important for the recruitment of neural stem cells to the ischemic brain (Andres et al., 2011). In hemorrhagic stroke, we found that deletion of CCL2 or CCR2 significantly decreased the injury volume and brain edema and enhanced neurological deficit score at early time points, but delayed the recovery and clearance of the hematoma. Consistent with the ischemic studies, our data also support such a complex role of the CCL2-CCR2 system in ICH. The early beneficial role of lack of CCL2 is probably due to decreased cytokine & chemokine secretion, leading to attenuated neuronal death. The delayed recovery, however, may be caused by the dysregulation of inflammatory response. The activation of alternative chemokine signaling pathways and over-activation/accumulation of microglia/macrophages may prolong the detrimental phase of inflammation or prevent the transition from detrimental phase to beneficial phase. Thus, further investigations should focus on the time course of CCL2-CCR2 activation, the compensation of inhibiting CCL2-CCR2 activation, and the potential molecular mechanisms regulating its expression.

Supplementary Material

Refer to Web version on PubMed Central for supplementary material.

Acknowledgments

We thank Dr M. Frohman and Tsirka lab members for advice and discussions. This work was partially supported by a SigmaXi grant-in-aid (to YY) and NIH R0142168 (to SET).

References

Andres RH, Choi R, Pendharkar AV, Gaeta X, Wang N, Nathan JK, Chua JY, Lee SW, Palmer TD, Steinberg GK, Guzman R. The CCR2/CCL2 Interaction Mediates the Transendothelial Recruitment of Intravascularly Delivered Neural Stem Cells to the Ischemic Brain. Stroke. 2011

Bian GL, Wei LC, Shi M, Wang YQ, Cao R, Chen LW. Fluoro-Jade C can specifically stain the degenerative neurons in the substantia nigra of the 1-methyl-4-phenyl-1,2,3,6-tetrahydro pyridine-treated C57BL/6 mice. Brain Res. 2007; 1150:55–61. [PubMed: 17397812]

Candelario-Jalil E, Gonzalez-Falcon A, Garcia-Cabrera M, Leon OS, Fiebich BL. Post-ischaemic treatment with the cyclooxygenase-2 inhibitor nimesulide reduces blood-brain barrier disruption and leukocyte infiltration following transient focal cerebral ischaemia in rats. J Neurochem. 2007; 100:1108–1120. [PubMed: 17176264]

Castillo J, Davalos A, Alvarez-Sabin J, Pumar JM, Leira R, Silva Y, Montaner J, Kase CS. Molecular signatures of brain injury after intracerebral hemorrhage. Neurology. 2002; 58:624–629. [PubMed: 11865143]

Cavcic A, Tesovic G, Gorenec L, Grgic I, Benic B, Lepej SZ. Concentration gradient of CXCL10 and CXCL11 between the cerebrospinal fluid and plasma in children with enteroviral aseptic meningitis. Eur J Paediatr Neurol. 2011

Clark W, Gunion-Rinker L, Lessov N, Hazel K. Citicoline treatment for experimental intracerebral hemorrhage in mice. Stroke. 1998; 29:2136–2140. [PubMed: 9756595]

Dimitrijevic OB, Stamatovic SM, Keep RF, Andjelkovic AV. Effects of the chemokine CCL2 on blood-brain barrier permeability during ischemia-reperfusion injury. J Cereb Blood Flow Metab. 2006; 26:797–810. [PubMed: 16192992]

Dimitrijevic OB, Stamatovic SM, Keep RF, Andjelkovic AV. Absence of the chemokine receptor CCR2 protects against cerebral ischemia/reperfusion injury in mice. Stroke. 2007; 38:1345–1353. [PubMed: 17332467]

Donnan GA, Hankey GJ, Davis SM. Intracerebral haemorrhage: a need for more data and new research directions. Lancet Neurol. 2010; 9:133–134. [PubMed: 20056490]

Elkabes S, DiCicco-Bloom EM, Black IB. Brain microglia/macrophages express neurotrophins that selectively regulate microglial proliferation and function. J Neurosci. 1996; 16:2508–2521. [PubMed: 8786427]

Gong C, Boulis N, Qian J, Turner DE, Hoff JT, Keep RF. Intracerebral hemorrhage-induced neuronal death. Neurosurgery. 2001; 48:875–882. discussion 882–873. [PubMed: 11322448]

Gong C, Hoff JT, Keep RF. Acute inflammatory reaction following experimental intracerebral hemorrhage in rat. Brain Res. 2000; 871:57–65. [PubMed: 10882783]

Gurney KJ, Estrada EY, Rosenberg GA. Blood-brain barrier disruption by stromelysin-1 facilitates neutrophil infiltration in neuroinflammation. Neurobiol Dis. 2006; 23:87–96. [PubMed: 16624562]

Kim SU, de Vellis J. Microglia in health and disease. J Neurosci Res. 2005; 81:302–313. [PubMed: 15954124]

Kooij G, Mizee MR, van Horssen J, Reijerkerk A, Witte ME, Drexhage JA, van der Pol SM, van Het Hof B, Scheffer G, Scheper R, Dijkstra CD, van der Valk P, de Vries HE. Adenosine triphosphate-binding cassette transporters mediate chemokine (C-C motif) ligand 2 secretion from reactive astrocytes: relevance to multiple sclerosis pathogenesis. Brain. 2011; 134:555–570. [PubMed: 21183485]

Kuang Y, Lackay SN, Zhao L, Fu ZF. Role of chemokines in the enhancement of BBB permeability and inflammatory infiltration after rabies virus infection. Virus Res. 2009; 144:18–26. [PubMed: 19720239]

Lortat-Jacob H, Grosdidier A, Imberty A. Structural diversity of heparan sulfate binding domains in chemokines. Proc Natl Acad Sci U S A. 2002; 99:1229–1234. [PubMed: 11830659]

Ma Q, Manaenko A, Khatibi NH, Chen W, Zhang JH, Tang J. Vascular adhesion protein-1 inhibition provides antiinflammatory protection after an intracerebral hemorrhagic stroke in mice. J Cereb Blood Flow Metab. 2011; 31:881–893. [PubMed: 20877383]

Matsushita K, Meng W, Wang X, Asahi M, Asahi K, Moskowitz MA, Lo EH. Evidence for apoptosis after intercerebral hemorrhage in rat striatum. J Cereb Blood Flow Metab. 2000; 20:396–404. [PubMed: 10698078]

Moxon-Emre I, Schlichter LC. Neutrophil depletion reduces blood-brain barrier breakdown, axon injury, and inflammation after intracerebral hemorrhage. J Neuropathol Exp Neurol. 2011; 70:218–235. [PubMed: 21293296]

Nelson TE, Hao C, Manos J, Ransohoff RM, Gruol DL. Altered hippocampal synaptic transmission in transgenic mice with astrocyte-targeted enhanced CCL2 expression. Brain Behav Immun. 2011; 25(Suppl 1):S106–119. [PubMed: 21356306]

Peeling J, Yan HJ, Corbett D, Xue M, Del Bigio MR. Effect of FK-506 on inflammation and behavioral outcome following intracerebral hemorrhage in rat. Exp Neurol. 2001; 167:341–347. [PubMed: 11161622]

Provencio JJ, Altay T, Smithason S, Moore SK, Ransohoff RM. Depletion of Ly6G/C(+) cells ameliorates delayed cerebral vasospasm in subarachnoid hemorrhage. J Neuroimmunol. 2011; 232:94–100. [PubMed: 21059474]

Qureshi JA, Notta NJ, Salahuddin N, Zaman V, Khan JA. An epidemic of Dengue fever in Karachi--associated clinical manifestations. J Pak Med Assoc. 1997; 47:178–181. [PubMed: 9301157]

Reijerkerk A, Kooij G, van der Pol SM, Leyen T, van Het Hof B, Couraud PO, Vivien D, Dijkstra CD, de Vries HE. Tissue-type plasminogen activator is a regulator of monocyte diapedesis through the brain endothelial barrier. J Immunol. 2008; 181:3567–3574. [PubMed: 18714030]

Ribo M, Grotta JC. Latest advances in intracerebral hemorrhage. Curr Neurol Neurosci Rep. 2006; 6:17–22. [PubMed: 16469266]

Schmued LC, Albertson C, Slikker W Jr. Fluoro-Jade: a novel fluorochrome for the sensitive and reliable histochemical localization of neuronal degeneration. Brain Res. 1997; 751:37–46. [PubMed: 9098566]

Schmued LC, Hopkins KJ. Fluoro-Jade B: a high affinity fluorescent marker for the localization of neuronal degeneration. Brain Res. 2000; 874:123–130. [PubMed: 10960596]

Semple BD, Frugier T, Morganti-Kossmann MC. CCL2 modulates cytokine production in cultured mouse astrocytes. J Neuroinflammation. 2010; 7:67. [PubMed: 20942978]

Sheehan JJ, Zhou C, Gravanis I, Rogove AD, Wu YP, Bogenhagen DF, Tsirka SE. Proteolytic activation of monocyte chemoattractant protein-1 by plasmin underlies excitotoxic neurodegeneration in mice. J Neurosci. 2007; 27:1738–1745. [PubMed: 17301181]

Stamatovic SM, Dimitrijevic OB, Keep RF, Andjelkovic AV. Protein kinase Calpha-RhoA cross-talk in CCL2-induced alterations in brain endothelial permeability. J Biol Chem. 2006; 281:8379–8388. [PubMed: 16439355]

Stamatovic SM, Keep RF, Kunkel SL, Andjelkovic AV. Potential role of MCP-1 in endothelial cell tight junction ‘opening’: signaling via Rho and Rho kinase. J Cell Sci. 2003; 116:4615–4628. [PubMed: 14576355]

Stamatovic SM, Shakui P, Keep RF, Moore BB, Kunkel SL, Van Rooijen N, Andjelkovic AV. Monocyte chemoattractant protein-1 regulation of blood-brain barrier permeability. J Cereb Blood Flow Metab. 2005; 25:593–606. [PubMed: 15689955]

Thiex R, Mayfrank L, Rohde V, Gilsbach JM, Tsirka SA. The role of endogenous versus exogenous tPA on edema formation in murine ICH. Exp Neurol. 2004; 189:25–32. [PubMed: 15296833]

Thompson WL, Van Eldik LJ. Inflammatory cytokines stimulate the chemokines CCL2/MCP-1 and CCL7/MCP-3 through NFkB and MAPK dependent pathways in rat astrocytes [corrected]. Brain Res. 2009; 1287:47–57. [PubMed: 19577550]

Tsukuda K, Mogi M, Iwanami J, Min LJ, Jing F, Oshima K, Horiuchi M. Irbesartan attenuates ischemic brain damage by inhibition of MCP-1/CCR2 signaling pathway beyond AT receptor blockade. Biochem Biophys Res Commun. 2011; 409:275–279. [PubMed: 21575596]

Wang J. Preclinical and clinical research on inflammation after intracerebral hemorrhage. Prog Neurobiol. 2010; 92:463–477. [PubMed: 20713126]

Wang J, Dore S. Inflammation after intracerebral hemorrhage. J Cereb Blood Flow Metab. 2007; 27:894–908. [PubMed: 17033693]

Wang J, Rogove AD, Tsirka AE, Tsirka SE. Protective role of tuftsin fragment 1–3 in an animal model of intracerebral hemorrhage. Ann Neurol. 2003; 54:655–664. [PubMed: 14595655]

Wang J, Tsirka SE. Neuroprotection by inhibition of matrix metalloproteinases in a mouse model of intracerebral haemorrhage. Brain. 2005a; 128:1622–1633. [PubMed: 15800021]

Wang J, Tsirka SE. Tuftsin fragment 1–3 is beneficial when delivered after the induction of intracerebral hemorrhage. Stroke. 2005b; 36:613–618. [PubMed: 15692122]

Xi G, Keep RF, Hoff JT. Mechanisms of brain injury after intracerebral haemorrhage. Lancet Neurol. 2006; 5:53–63. [PubMed: 16361023]

Xue M, Del Bigio MR. Intracerebral injection of autologous whole blood in rats: time course of inflammation and cell death. Neurosci Lett. 2000a; 283:230–232. [PubMed: 10754230]

Xue M, Del Bigio MR. Intracortical hemorrhage injury in rats : relationship between blood fractions and brain cell death. Stroke. 2000b; 31:1721–1727. [PubMed: 10884479]

Yao Y, Tsirka SE. The C terminus of mouse monocyte chemoattractant protein 1 (MCP1) mediates MCP1 dimerization while blocking its chemotactic potency. J Biol Chem. 2010; 285:31509–31516. [PubMed: 20682771]

Yao Y, Tsirka SE. Mouse MCP1 C-terminus inhibits human MCP1-induced chemotaxis and BBB compromise. J Neurochem. 2011a; 118:215–223. [PubMed: 21615737]

Yao Y, Tsirka SE. Truncation of monocyte chemoattractant protein 1 by plasmin promotes blood-brain barrier disruption. J Cell Sci. 2011b; 124:1486–1495. [PubMed: 21486949]

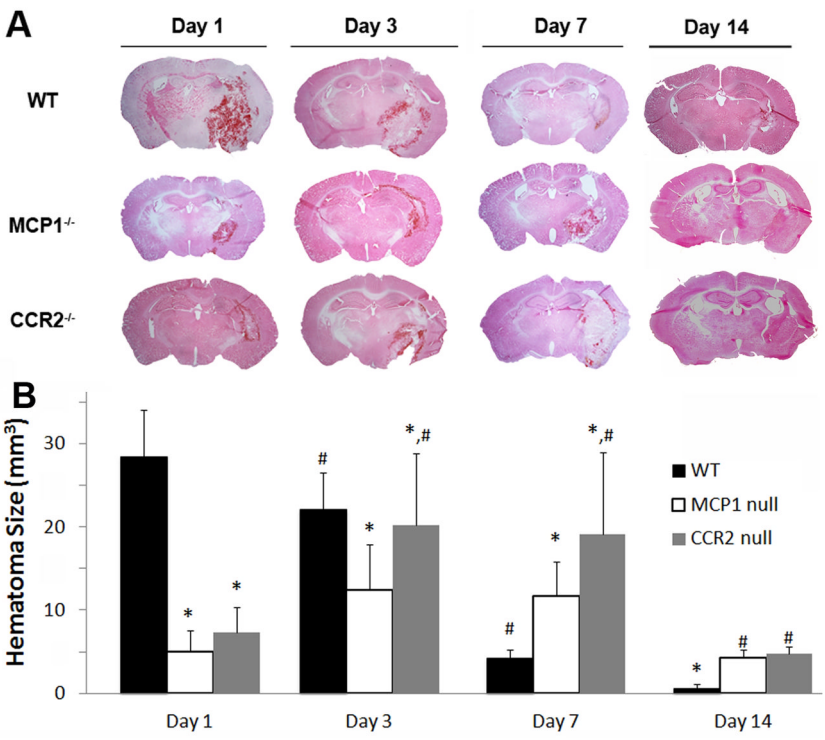

Figure 1. The effect of CCL2 or CCR2 on injury volume

A. Wild-type, CCL2$^{-/-}$, and CCR2$^{-/-}$ mice were injected with collagenase and the injury volume was examined by H&E staining 0, 1, 3, 7, and 14 days later. **B.** Quantitative data of injury volume are mean±SD (n=4–7).

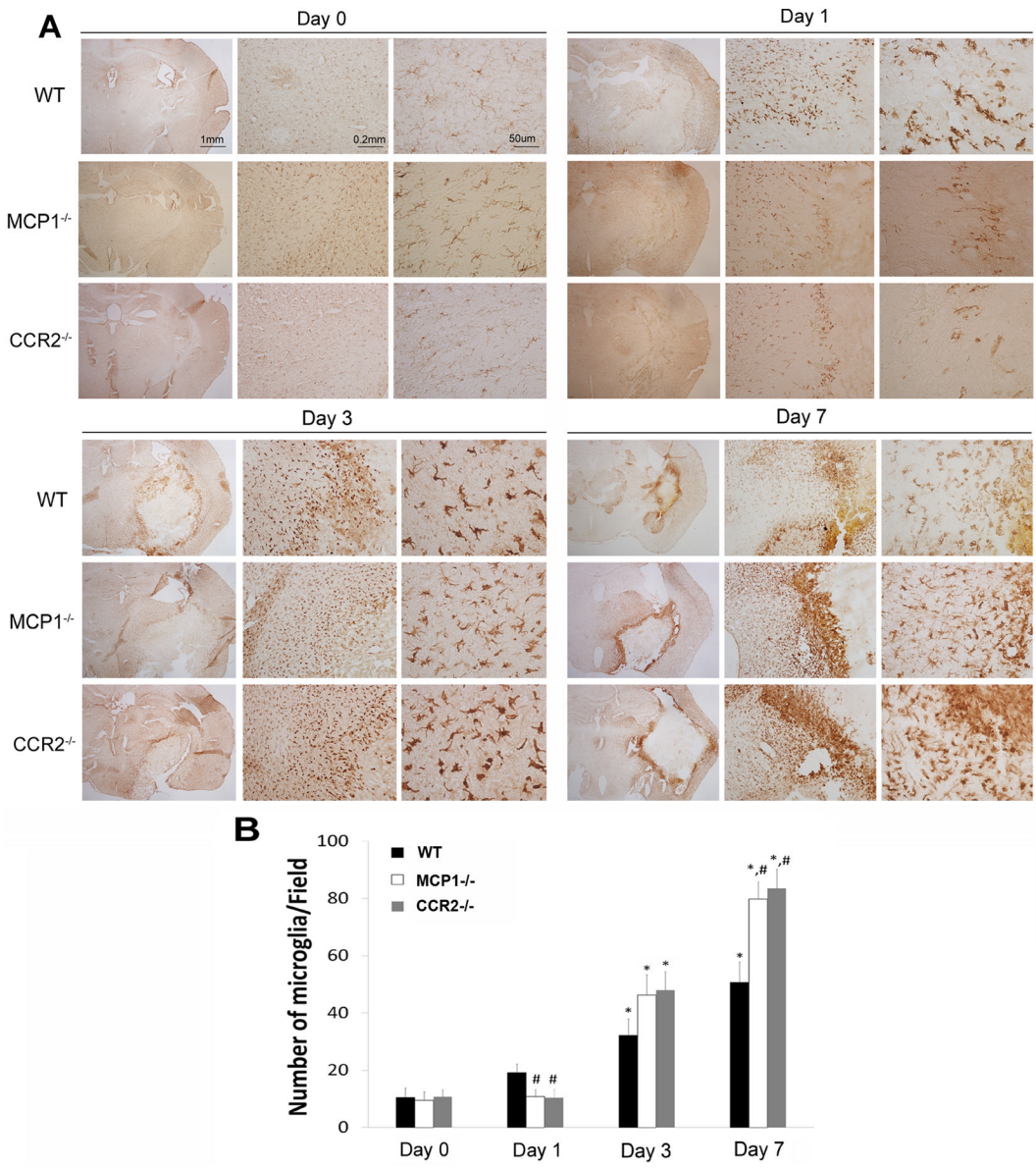

Figure 2. CCL2 and CCR2 deficiency affects microglial/macrophage activation after ICH

A. Wild-type, CCL2$^{-/-}$, and CCR2$^{-/-}$ mice before (day 0), or after ICH (1, 3, 7 dpi) were perfused, and microglial/macrophage activation was examined by Iba-1 DAB-staining. **B.** Quantitative data of Iba-1^{+} cells. Data are shown as mean±SD (n=4).

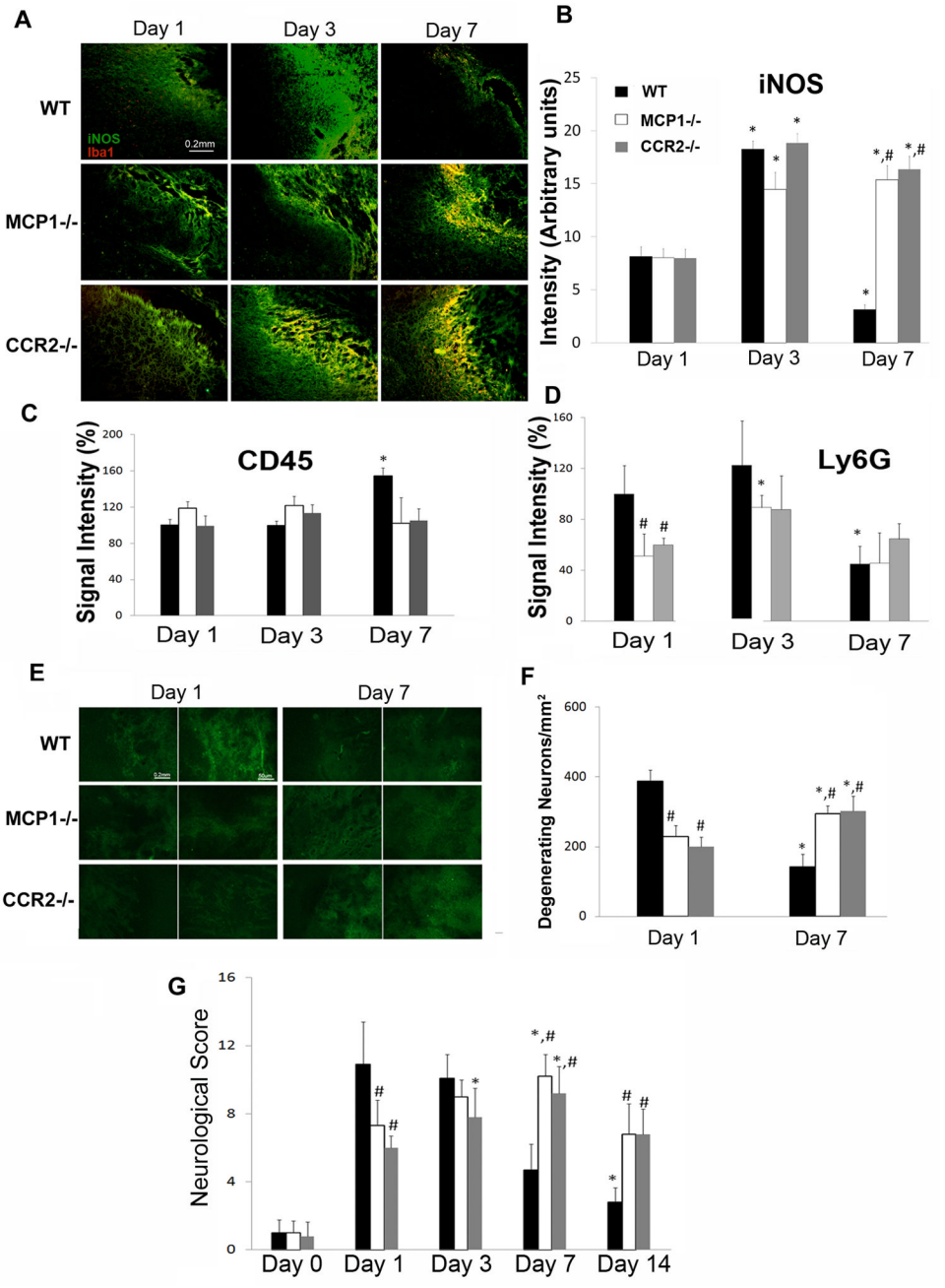

Figure 3. CCL2 and CCR2 deficiency on iNOS expression, leukocyte infiltration, neuronal death, and neurological behavior

A. Wild-type, CCL2$^{-/-}$, and CCR2$^{-/-}$ mice were injected with collagenase and Iba-1 (red) and iNOS (green) levels were assessed 1, 3, 7dpi. **B.** Quantitative data of iNOS (mean pixel intensity) levels are mean±SD (n=3). **C and D.** The infiltration of leukocytes and neutrophils was examined using CD45 (**C**) and Ly6G (**D**) immunostaining, respectively, at 1, 3, 7dpi. Data are mean±SD (n=4). **E.** Representative images of Flour Jade C staining. **F.** Quantification of the number of degenerating neurons on days 1 and 7dpi. Data are mean ±SD (n=4). **G.** Neurological scores were evaluated at 1, 3, and 7dpi. Values are mean±SD. The animal numbers for wt, CCL2$^{-/-}$, and CCR2$^{-/-}$ at 1, 3, 7dpi were 17, 8, 13; 16, 7, 6; and 9, 12, 5, respectively.

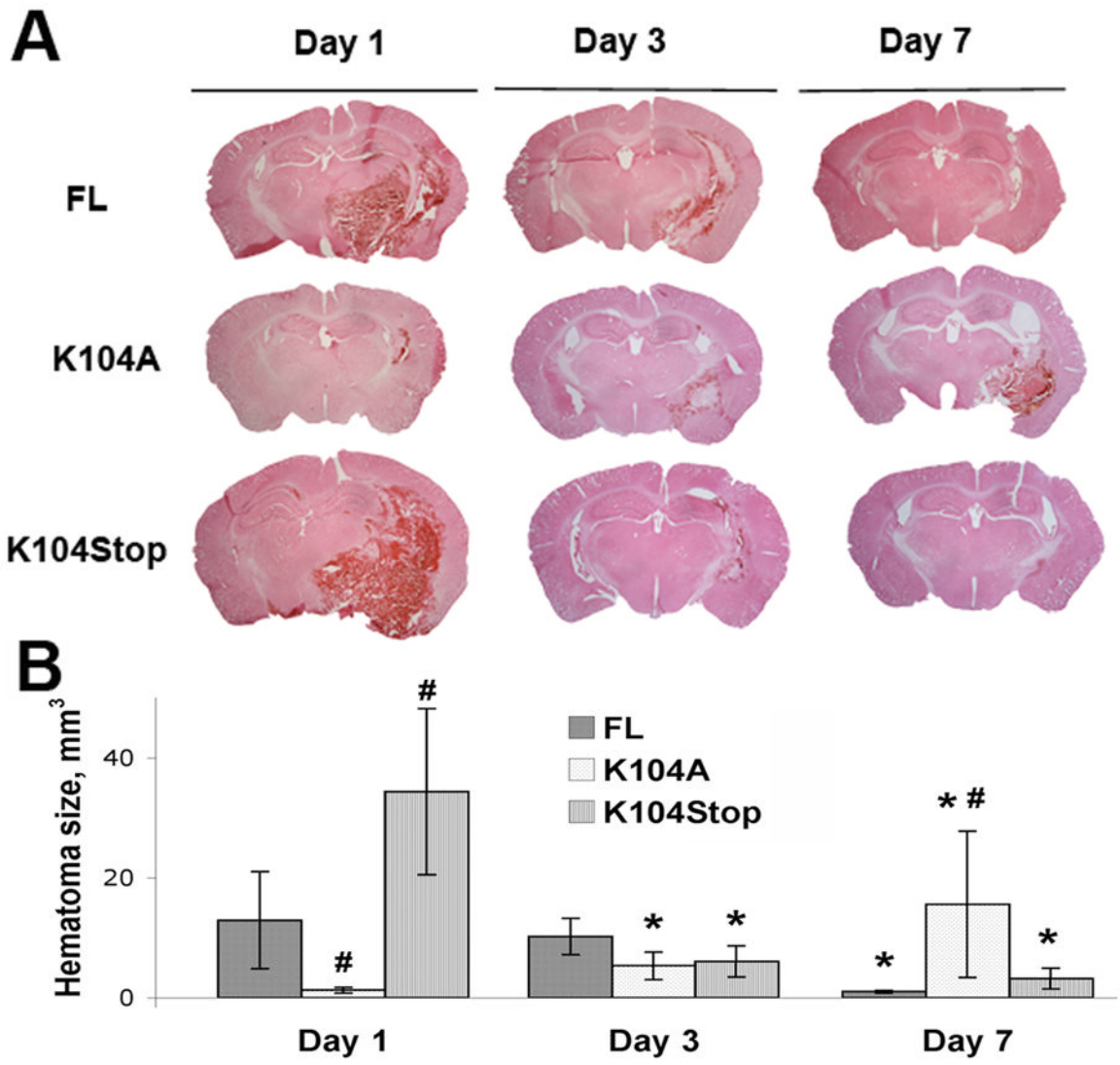

Figure 4. The effect of recombinant CCL2 proteins on injury volume

A. CCL2$^{-/-}$ mice were injected with collagenase and FL-, K104A-, or K104Stop-CCL2 and the injury volume was examined by H&E staining 1, 3, 7dpi. **B.** Quantitative data of injury volume are mean±SD (n=4).

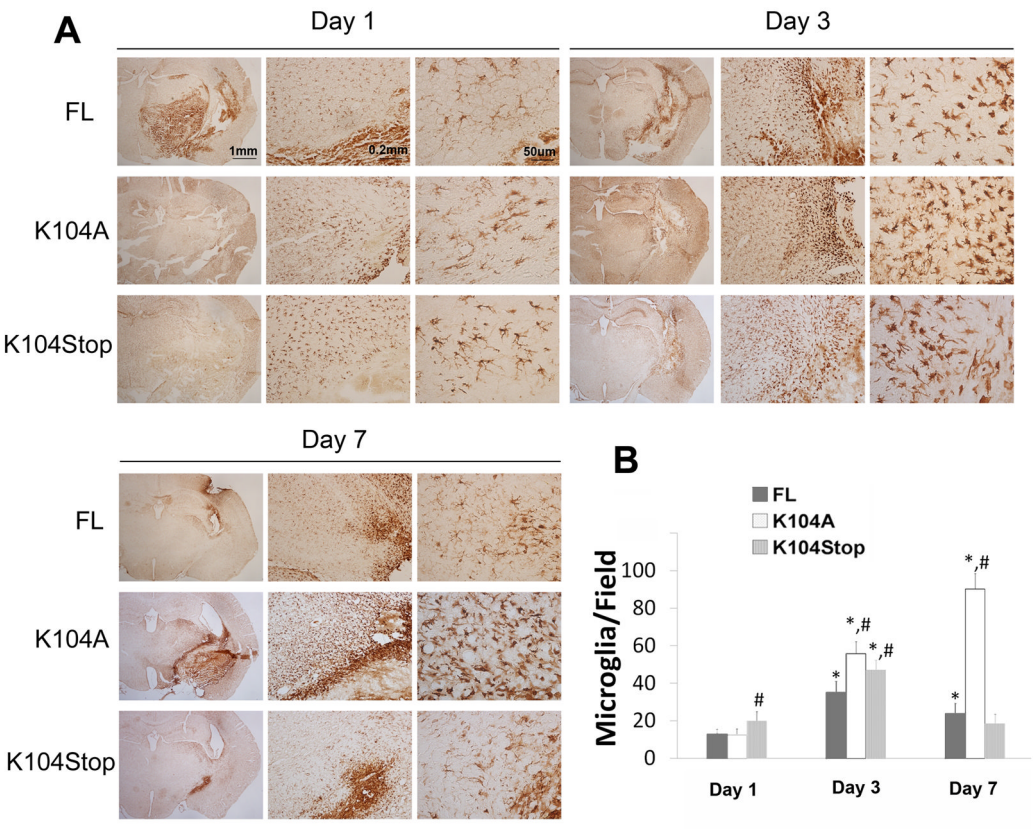

Figure 5. Recombinant CCL2 proteins change microglial/macrophage activation pattern after ICH

A. $CCL2^{-/-}$ mice were injected with collagenase and FL-, K104A-, or K104Stop-CCL2. The brains were collected at 1, 3, 7 dpi and DAB-stained with Iba-1 antibody. **B.** Quantitative data of Iba-1^{+} cells. Data are shown as mean±SD (n=4).

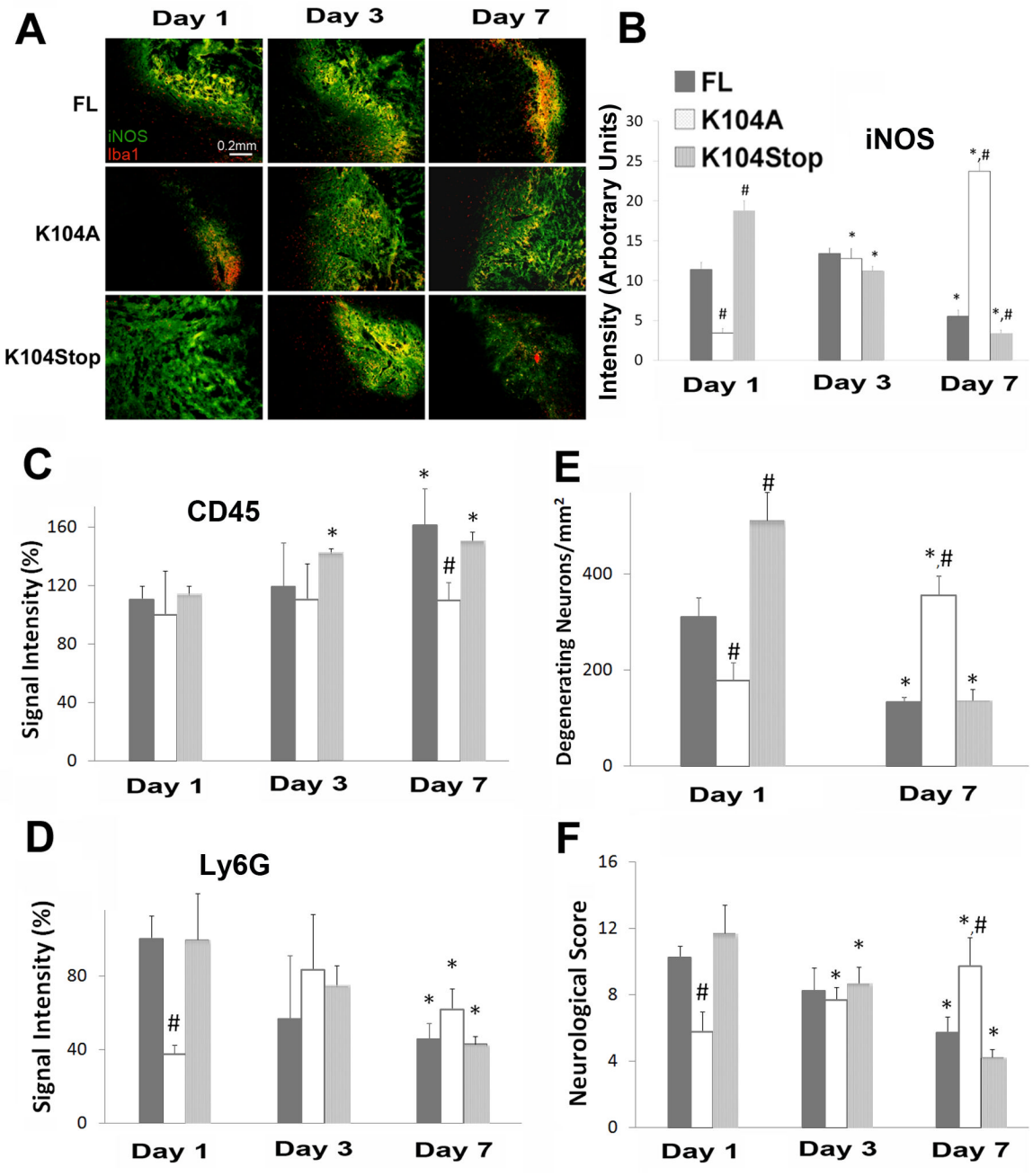

Figure 6. Recombinant CCL2 proteins rescue ICH properties in CCL2$^{-/-}$ mice

A. CCL2$^{-/-}$ mice were injected with collagenase and FL-, K104A-, or K104Stop-CCL2. 1, 3, 7dpi the brains were collected and stained for Iba-1 and iNOS. **B.** Quantitative data of iNOS (mean pixel intensity) are mean±SD (n=3). **C and D.** The infiltration of leukocytes and neutrophils was examined using CD45 (**C**) and Ly6G (**D**) immunostaining, respectively, at 1, 3, 7dpi. Data are mean±SD (n=4). **E.** Degenerating neurons were visualized using FluoroJade C on days 1 and 7dpi and quantified. Data are mean±SD (n=3). **F.** Neurological scores were evaluated at 1, 3, and 7dpi. Values are mean±SD. The animal numbers for CCL2$^{-/-}$ mice infused with FL, K104A, and K104Stop-CCL2 at 1, 3, 7dpi were 8, 8, 3; 9, 6, 4; and 11, 6, 3, respectively.

Table 1

Edema after ICH

A. Wild-type, CCL2$^{-/-}$, and CCR2$^{-/-}$ mice were subjected to ICH and water content was calculated, as described in Materials and Methods. Data are mean±SD (n=6).

Genotype (time post ICH)		Water content (%)		
		Contralateral	Ipsilateral	Cerebellum
Wt	Day 1	76.67±0.24	79.67±0.82	74.48±0.71
	Day 3	76.92±0.57	78.9±0.62	74.94±0.75
	Day 7	76.43±0.85	77.04±0.92*	74.39±1.97
CCL2$^{-/-}$	Day 1	76.55±0.64	77.87±0.50$^{\#}$	74.73±0.66
	Day 3	76.53±0.29	78.52±0.36	74.89±0.30
	Day 7	76.81±0.64	78.90±0.30*,$^{\#}$	74.95±0.36
CCR2$^{-/-}$	Day 1	76.80±0.32	78.11±0.28$^{\#}$	74.58±0.30
	Day 3	76.81±0.48	78.63±0.60	74.91±0.50
	Day 7	76.56±0.45	79.73±0.84*,$^{\#}$	74.83±0.63

B. CCL2$^{-/-}$ mice were injected with collagenase and FL-, K104A-, or K104Stop-CCL2. The water content was calculated at 1, 3 and 7dpi. Data are shown as mean±SD (n=3).

Treatment (time post ICH)		Water content (%)		
		Contralateral	Ipsilateral	Cerebellum
FL CCL2	Day 1	76.63±0.27	78.52±0.30	74.63±0.23
	Day 3	76.56±0.33	78.45±0.34	74.67±0.04
	Day 7	76.57±0.34	77.20±0.28*	74.58±0.22
K104A CCL2	Day 1	76.45±0.34	77.24±0.26$^{\#}$	74.63±0.33
	Day 3	76.35±0.26	77.34±0.29$^{\#}$	74.66±0.09
	Day 7	76.51±0.30	78.64±0.24*,$^{\#}$	74.60±0.23
K104Stop CCL2	Day 1	76.73±0.21	80.11±0.70$^{\#}$	74.60±0.10
	Day 3	76.73±0.50	77.25±0.06*,$^{\#}$	74.63±0.25
	Day 7	76.37±0.25	77.03±0.09*	74.63±0.12